Charge-carrier relaxation in disordered organic semiconductors studied by dark injection: Experiment and modeling

M. Mesta,[1] C. Schaefer,[1,2] J. de Groot,[1] J. Cottaar,[1] R. Coehoorn,[1,2] and P. A. Bobbert[1]
[1]*Department of Applied Physics, Technische Universiteit Eindhoven, P.O. Box 513, NL-5600 MB Eindhoven, The Netherlands*
[2]*Philips Research Laboratories, High Tech Campus 4, NL-5656 AE Eindhoven, The Netherlands*
(Received 30 August 2013; published 26 November 2013)

Understanding of stationary charge transport in disordered organic semiconductors has matured during recent years. However, charge-carrier relaxation in nonstationary situations is still poorly understood. Such relaxation can be studied in dark injection experiments, in which the bias applied over an unilluminated organic semiconductor device is abruptly increased. The resulting transient current reveals both charge-carrier transport and relaxation characteristics. We performed such experiments on hole-only devices of a polyfluorene-based organic semiconductor. Modeling the dark injection by solving a one-dimensional master equation using the equilibrium carrier mobility leads to a too-slow current transient, since this approach does not account for carrier relaxation. Modeling by solving a three-dimensional time-dependent master equation does take into account all carrier transport and relaxation effects. With this modeling, the time scale of the current transient is found to be in agreement with experiment. With a disorder strength somewhat smaller than extracted from the temperature-dependent stationary current-voltage characteristics, also the shape of the experimental transients is well described.

DOI: 10.1103/PhysRevB.88.174204 PACS number(s): 72.20.Ee, 72.80.Le, 73.61.Ph, 81.05.Fb

I. INTRODUCTION

In the understanding of the functioning of organic semiconductor devices, such as organic light-emitting diodes (OLEDs), knowledge about the various aspects of the charge dynamics in these devices is crucial. In recent years, much progress has been made in measuring and modeling the charge-carrier mobility μ in such devices under stationary conditions. Key to a proper description of charge transport is the energetic disorder present in the organic semiconductors used in these devices. This disorder is commonly described by assuming that carriers hop between sites having random energies, which are often assumed to be distributed according to a Gaussian density of states (DOS) with a standard deviation σ, henceforth called the "disorder strength." The resulting model is called the Gaussian disorder model.[1] At increasing carrier densities state-filling effects come into play, leading to a dependence of μ on the charge-carrier concentration c.[2–5] Together with the dependence of the mobility on temperature, T, and electric field, F, this has led to the extended Gaussian disorder model (EGDM). A parametrization of the mobility function $\mu(T,c,F)$ within the EGDM was constructed in Ref. 5. It has been proposed that spatial correlation in the energies of the sites can be present, for example due to the presence of dipoles,[6,7] leading to the correlated disorder model. When also in this model the density dependence is included, this results in the extended correlated disorder model (ECDM).[8]

Charge transport in organic semiconductors can be studied in single-carrier devices, in which carrier-injecting electrodes are used with work functions that are close to either the highest occupied molecular orbital (HOMO) or the lowest unoccupied molecular orbital of the semiconductor. By this it is possible to study the transport of holes and electrons separately. By modeling the current density-voltage, J-V, characteristics of such devices using different mobility functions, one can extract values for the disorder strength σ and the density of sites, N_t, and judge whether the EGDM or ECDM provides the most appropriate mobility function. It has been found that charge transport in two typical small-molecule semiconductors, N,N'-di(naphthalen-1-yl)-N,N'-diphenyl-benzidine (α-NPD)[9] (a hole conductor) and bis(2-methyl-8-quinolinato)-4-phenylphenolate aluminum (BAlq)[10] (an electron conductor), can be described most appropriately with the ECDM. On the other hand, charge transport in polymeric semiconductors like two Poly-(p-phenylene vinylene) (PPV)-based polymers[5,8] (hole transport) and a polyfluorene-based polymer[11,12] (hole and electron transport) can be described best with the EGDM. Description of electron transport requires the consideration of traps, which makes the analysis more involved.[10,12]

However, studies of stationary properties like J-V characteristics can provide only a limited insight into charge dynamics, because they do not address the possible time dependence of the charge transport. A large body of work exists on the time dependence of charge transport in disordered, organic and inorganic, solids. The standard technique to study time-dependent transport is a time-of-flight (TOF) experiment, where in a sandwich device of a disordered solid a sheet of carriers is photogenerated at one of the electrodes, after which the carriers move to the opposite collecting electrode in an applied electric field. Dispersion in the transport leads to different carrier arrival times at the collecting electrode, resulting in a smoothly instead of abruptly decaying current transient. Such transients are often described in terms of the Scher-Montroll theory,[13] which has, for example, been quite successfully applied in the case of a molecularly doped polymer.[14] In the case of semiconducting polymers TOF experiments can be used to extract the carrier mobility and its dependence on temperature and electric field.[15] The effect of relaxation of an excitation in the DOS of localized states[16] has also been analyzed with TOF experiments.[17] A difficulty with TOF experiments, however, is that relatively thick ($\sim$1 μm or more) layers should be used to make sure

that the photogeneration occurs in a region that is narrow as compared to the total device thickness. This makes the TOF experiment unsuitable for studying time-dependent transport in the relatively thin devices (∼100 nm) that are of importance for OLED studies.

Alternative techniques to study time-dependent transport in thin devices are available. Recently, impedance-spectroscopy studies were performed on hole-only devices of a polyfluorene-based polymer (the same as in Refs. 11 and 12), with a thickness around 100 nm, showing the importance of carrier-relaxation effects.[18] A fair description of the frequency- and voltage-dependent capacitance could be obtained within a one-dimensional (1D) multiple-trapping model for carrier relaxation.[18] In that study, the following approach was used: (1) three-dimensional (3D) Monte Carlo (MC) calculations were carried out to obtain the time-dependent mobility after a sudden very small increase of the charge density, providing the (complex) frequency-dependent mobility after a Fourier transformation, and (2) this result was included in a 1D calculation of the (complex) frequency-dependent current density. Because this approach is indirect and rather involved, it is of interest to analyze the results of transient current-density measurements using a more direct fully 3D approach.

Here, we extend the study of carrier-relaxation effects by performing and analyzing so-called dark-injection (DI) experiments on these hole-only devices. In DI experiments the bias applied over an unilluminated semiconductor device is abruptly increased and the current transient as a function of time is recorded. Because instantaneous injection of extra charges occurs by the bias step, DI experiments are in spirit comparable to TOF experiments. However, DI experiments are more flexible, because they can be applied to thinner devices. Furthermore, they are applicable to situations with much higher carrier densities, outside the independent-particle Boltzmann regime, as is relevant to, for example, OLED applications. DI experiments were used extensively to study charge transport in OLEDs by Poplavskyy *et al.*[19–21] An early theoretical description of DI transients was given by Many and Rakavy.[22] In their description, space-charge effects are taken into account, but the mobility μ is assumed constant; i.e., no dependence of μ on carrier density and electric field is taken into account and there is no relaxation. Also, diffusion is not accounted for. Within this description a peak in the transient current occurs at a time $t_{\mathrm{peak}} = 0.786\, t_{\mathrm{SCF}}$, where t_{SCF} is the space charge-free carrier transit time. The latter is given by $t_{\mathrm{SCF}} = L^2/\mu V$, where L is the thickness of the device and V the applied voltage. An improvement of the Many-Rakavy theory, applicable to organic semiconductor devices, was provided by Knapp and Ruhstaller by using the carrier-density and field dependence of μ from the EGDM.[23] In their description, the 1D time-dependent drift-diffusion (DD) equation for the carrier density is solved in conjunction with the 1D Poisson equation for the electric field, with the diffusion coefficient obtained from the mobility via the generalized Einstein equation.[24] These authors recently applied their technique to the study of traps.[25] Their 1D DD approach is presently considered to be the state of the art in DI modeling. In the present work we instead use an approach in which a time-dependent 1D master equation (ME) is solved, which treats drift and diffusion on equal footing.[26] Results obtained with this approach are very similar to those obtained from the 1D DD equation, but the application of the 1D ME approach is more convenient and simple.[26] However, neither the 1D DD nor the 1D ME approach accounts for carrier relaxation.

Instead of using the indirect multiple-trapping model of Ref. 18 to take into account relaxation effects, we follow here a direct and more fundamental approach in which the 3D time-dependent master equation for the occupational probabilities of a system of hopping sites representing the full device, including the injecting and collecting electrodes, is solved. This approach was very recently for the first time applied in the calculation of DI transients by Szymański *et al.*[27] The approach followed by us is in essence an extension of the stationary full-device ME calculations earlier explored by us[28] to include time dependence. We benchmark these 3D ME calculations with 3D MC simulations on the same hopping system, which are only feasible for thin devices and high voltages. In these simulations all effects of Coulomb interactions can be taken into account, whereas in the 3D ME calculations the Coulomb interactions can only be taken into account in a layer-averaged way.[28] The difference turns out to be unimportant.

In Sec. II, we describe the DI experiments and present their results. We also present the J-V characteristics of the investigated devices, which are used to extract parameters for the DI modeling. The modeling approaches are described in Sec. III. In Sec. III A we describe the 1D ME, in Sec. III B the 3D ME, and in Sec. III C the 3D MC approach. In Sec. IV we present the modeling results and the comparison with the experiments. Section V contains a summary, discussion, and conclusion.

II. EXPERIMENT

The experimental setup to perform the DI measurements is shown in Fig. 1(a). A voltage $V(t)$ is applied over the device, which is placed in series with a load resistance of 100 Ω. The current through the device is determined by measuring the voltage over the load resistance. The voltage $V(t)$ consists of a pulse train as indicated in Fig. 1(b), which allows us to judge the reproducibility of the transients and to increase the signal-to-noise ratio. The load resistance was chosen large enough to allow an accurate measurement of the current, but still such that it only significantly influences the current for short times $t < 2 \times 10^{-6}$ s after the onset of a pulse, which is smaller than the times for which the interesting structures in the transients appear. The load resistance is taken into account in most of our modeling.

The studied hole-only devices have the structure glass, indium tin oxide (100 nm), PEDOT:PSS (100 nm), LEP, Pd (100 nm). The light-emitting polymer (LEP) consists of polyfluorene with copolymerized triarylamine units for hole transport (Lumation$^{\mathrm{TM}}$Blue series, supplied by Sumation Co., Ltd.); see the inset of Fig. 1(c). The devices are the same as those studied in Refs. 11, 29, and 18 and have three different LEP-layer thicknesses: $L = 67$, 98, and 122 nm, respectively. The surface area of all three devices is $A = 9 \times 10^{-6}$ m^2.

Without a voltage offset in the DI experiments, the off time needed to return to the initial state of the device before application of a next voltage pulse turned out to be prohibitively long. We attribute this to very slow trapping/detrapping of charge carriers by deep traps. With a finite offset voltage, however,

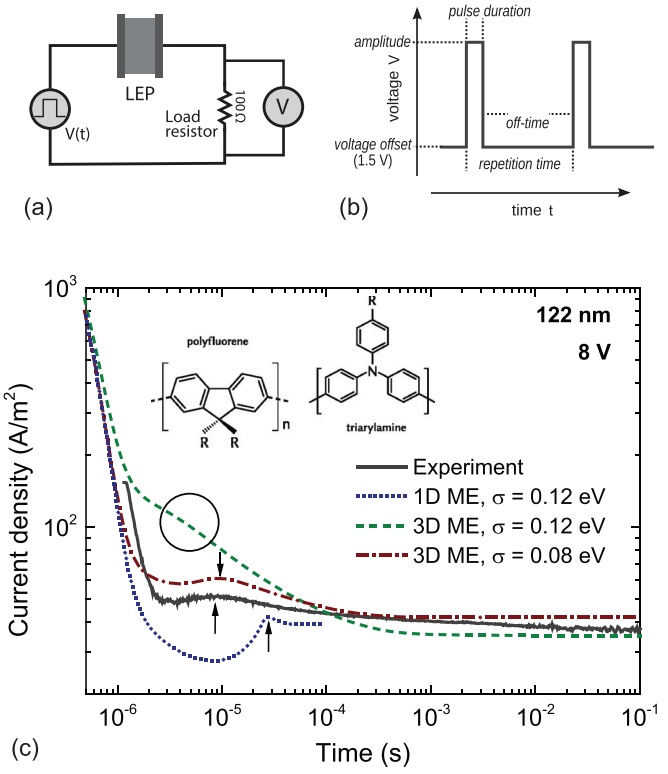

FIG. 1. (Color online) (a) Measurement setup for the dark-injection (DI) experiments. (b) Applied voltage pulse sequence. An offset voltage of 1.5 V is used. (c) DI transients for a device with a 122-nm-thick polymer layer and a pulse amplitude of 8 V. Solid lines, measurements; blue dotted lines, results of the one-dimensional master equation (1D ME) approach; green dashed and red dash-dotted lines, results of the three-dimensional master equation (3D ME) approach for two different values of the disorder strength σ. The arrows indicate the peak position in the transients, and the circle a shoulder in the 3D ME transient for $\sigma = 0.12$ eV. The error bars of all presented results are negligible. The inset in (c) shows the chemical structure of the used light-emitting polymer.

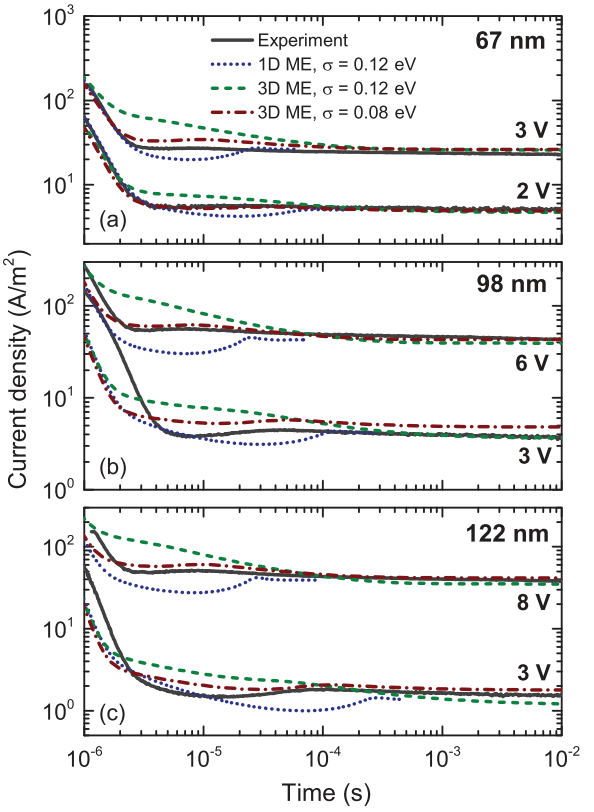

FIG. 2. (Color online) DI transients for different pulse amplitudes for devices with LEP-layer thicknesses of (a) $L = 67$, (b) $L = 98$, and (c) $L = 122$ nm. The parameters used in the 1D and 3D ME modeling are given in Table I. The transient presented in (c) for a pulse amplitude of 8 V is the same as in Fig. 1(c).

this can be circumvented. The reason is probably that the deep traps then remain filled and that the trapping/detrapping dynamics of the now relevant shallower traps is much faster. We chose to perform all experiments with an offset of 1.5 V, for which the reproducibility of the transients is very good. The shape of the transients was investigated as a function of the duty cycle (pulse duration as a fraction of the repetition time). The measurements discussed here were obtained with a duty cycle of 1%, for which memory effects were found to be negligible. The repetition frequencies ranged from 0.01 to 1 Hz, where the lower frequencies are needed for the measurements of the transients for longer times (10–800 ms).

A typical measured DI transient for the $L = 122$ nm device is given by the solid black line in Fig. 1(c) for a pulse amplitude of 8 V. The high current at short times is mostly due to the rapid charging of the device through the load resistance [the RC times of our devices are $(0.2–0.4)\times10^{-6}$ s]. The current then reaches a minimum at about 3×10^{-6} s, after which a maximum appears at about 8×10^{-6} s. This maximum, indicated by an arrow, is equivalent to the peak in the Many-Rakavy theory, signaling the arrival at the collecting contact (in this case the Pd electrode) of the front of the space charge injected at the onset of the voltage pulse by the injecting contact (in this case PEDOT:PSS). Finally, the current relaxes to the steady-state current at the pulse amplitude of 8 V. Figures 2(a), 2(b), and 2(c) give the transients for the $L = 67$, 98, and 122 nm devices, respectively, for different pulse amplitudes. The shapes of all transients are roughly equal, but the time at which the peak occurs depends on the pulse amplitude and the device thickness. The peak time as a function of voltage is plotted in Figs. 3(a)–3(c) for the three devices (black circles). The peak positions of transients at other voltages than those plotted in Fig. 2 were included in the data.

The current density-voltage (J-V) characteristics of the investigated three devices were measured in Ref. 11 for different temperatures. We remeasured the room-temperature J-V characteristics of the same devices and the results are displayed in Fig. 4. They show almost no difference from the results in Ref. 11, demonstrating that the devices are stable over at least 5 years.

III. THEORY AND SIMULATION

A. One-dimensional master equation

The approach in which the current is calculated by solving a 1D ME was introduced in Ref. 26. Within the 1D ME approach, drift and diffusion are both automatically included,

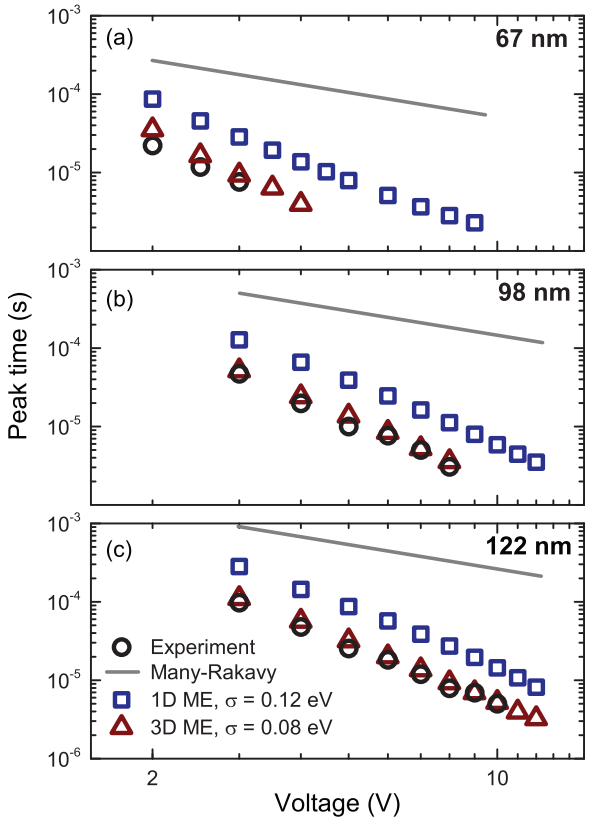

FIG. 3. (Color online) (a–c) Peak times [see arrows in Fig. 1(c)] as a function of pulse amplitude of the DI transients for devices with different LEP-layer thicknesses. Circles, experiments; gray lines, Many-Rakavy theory;[22] squares, 1D ME modeling results with $\sigma = 0.12$ eV; triangles, 3D ME modeling results with $\sigma = 0.08$ eV. The 3D ME transients with $\sigma = 0.12$ eV do not show a peak [see Figs. 1(c) and 2]. In addition to the transients shown in Fig. 2 also the peak times of transients at other pulse amplitudes were included.

in contrast to the approach in which the 1D DD equation is solved, in which drift and diffusion appear as separate terms. Charge transport in the 1D ME approach is described as nearest-neighbor hopping along a linear chain of discrete sites with a site separation a. The hopping rate is chosen such that the carrier-concentration-dependent mobility at zero electric field obtained from the EGDM[5] is reproduced. In the presence of an electric field, exponential hopping rate enhancement and suppression factors are included for down-field and up-field hops, respectively.

The carrier concentration c_i at site i satisfies the master equation

$$\frac{dc_i}{dt} = c_{i-1}r_i^+ + c_{i+1}r_{i+1}^- - c_i(r_{i+1}^+ + r_i^-), \qquad (1)$$

where $r_i^{+(-)}$ is the forward (backward) hopping rate across the interval from $i-1$ to i. The coupled master equations for all sites can be solved numerically by appropriate methods. The time-dependent electric field follows from Poisson's equation and evolves together with the carrier concentration. In this way, time-dependent space-charge effects are taken into account. After the time-dependent carrier concentrations have been found, the time-dependent current density is obtained

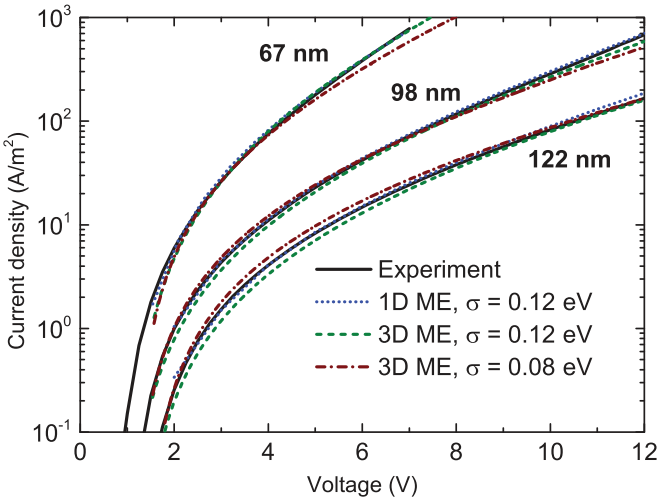

FIG. 4. (Color online) Current density versus voltage, J-V, characteristics of the three devices with different LEP-layer thicknesses. Fits to 1D and 3D ME modeling results lead to the parameters given in Table I.

from

$$J(t) = \sum_i (c_{i-1}r_i^+ - c_i r_i^-)\frac{e}{La^2} + \frac{\epsilon_0\epsilon_r}{L}\frac{dV}{dt}, \qquad (2)$$

where e is the electronic charge. The second term on the right-hand side is the displacement current density, where ϵ_0 is the vacuum permittivity and ϵ_r the relative dielectric constant of the LEP, which was determined to be $\epsilon_r = 3.2 \pm 0.1$.[11] In a stationary situation the left-hand side of the master equation Eq. (1) is zero and the displacement current density vanishes.

The effect of the load resistance can be accounted for without too much effort. The total applied voltage is a sum of the voltage drop over the device, V_{device}, and the load resistor, V_R. The latter is calculated using Ohm's law, $V_R = AJR$, after obtaining the current density in the device, J, from Eq. (2). Since the latter depends on V_{device}, an iterative procedure is followed. We note that carrier-relaxation effects are not included in the 1D ME approach: c_i represents the carrier concentration in a sheet and not the occupation of an actual site in the organic semiconductor. The effect of disorder on the transport is taken into account via the hopping rates r_i, as determined from 3D ME calculations under stationary conditions. They do not show the effective time dependence due to the presence of an out-of-equilibrium density of occupied states that arises under nonstationary conditions.

B. Three-dimensional master equation

Charge carrier-relaxation effects are included in the 3D ME approach. In this approach the LEP is represented by a regular cubic lattice with lattice constant a, where each lattice point is a site that can hold at most one charge carrier. Calculations of the stationary current density in complete single-carrier devices with the 3D ME approach were pioneered in Ref. 28. In a nonstationary situation a time dependence should be added to the occupational probabilities of the sites. In a simulation of a DI experiment, first the occupational probabilities of the sites are determined for the initially applied voltage in exactly the

same way as in Ref. 28. After the voltage step, the electric field in the device, and thus the energy of every site, has changed. As a result, the hopping rates between the sites have changed and the system is no longer in a stationary situation: extra carriers are injected from the injecting electrode into the adjacent organic sites and travel to the collecting electrode while relaxing to lower energies. Furthermore, the field becomes time dependent due to the time-dependent charge-carrier density. This requires extension of the approach of Ref. 28 to include time dependence, as described below.

The x direction of the simulation box is the direction of current flow. The size of the simulation box is $L \times L_y \times L_z$ and we use periodic boundary conditions in the y and z directions. For the lateral size of the simulation box we take $L_y = L_z = 50a$, which was found to be sufficient in steady-state ME calculations for similar devices.[28] The energies of the sites consist of a random contribution due to the energetic disorder in the polymer and a contribution due to the electric potential. The random contribution is chosen from a Gaussian DOS centered at the HOMO of the LEP:

$$g(E) = \frac{1}{\sqrt{2\pi}\sigma} \exp[-(E-\Delta)^2/2\sigma^2], \tag{3}$$

where the standard deviation σ of the Gaussian is the disorder parameter and Δ is an injection barrier with respect to the injecting contact (PEDOT:PSS).

We assume that charges hop between sites with a hopping rate given by the Miller-Abrahams formula[30]

$$W_{ij} = \nu_0 \exp[-2\alpha R_{ij}] \times \begin{cases} \exp[-\Delta E_{ij}/k_B T] & \text{if } \Delta E_{ij} > 0, \\ 1 & \text{if } \Delta E_{ij} < 0, \end{cases} \tag{4}$$

where the indices i and j denote the sites involved in the hopping, with mutual distance R_{ij}; the constant ν_0 is an intrinsic hopping rate, α the inverse wave function decay length, ΔE_{ij} the energy difference between the sites, and k_B Boltzmann's constant. We assume that the hopping takes places between nearest neighbors, so that $R_{ij} = a$. For α we take $10/a$, as in Ref. 5, but this value only influences the prefactor in the case of nearest-neighbor hopping. A small injection barrier of $\Delta = 0.1$ eV at the injecting contact, found in Ref. 11, is taken into account in our simulations.

The master equation governing the time dependence of the occupational probability p_i of a site i is now

$$\frac{dp_i}{dt} = \sum_{j \neq i} [W_{ji} p_j (1-p_i) - W_{ij} p_i (1-p_j)]. \tag{5}$$

A time-dependent electric field in the x direction is obtained by solving a one-dimensional Poisson equation, in which a layer-averaged charge density is taken that only depends on x. This is the way the effects of space charge are taken into account in the 3D ME approach.[28] After obtaining the p_i's by solving the coupled master equations of all sites, the current density is obtained from

$$J(t) = \frac{e}{L L_y L_z} \sum_{i,j} W_{ij} p_i (1-p_j) R_{ij,x} + \frac{\epsilon_0 \epsilon_r}{L} \frac{dV}{dt}, \tag{6}$$

where $R_{ij,x}$ is the x component of the vector between sites i and j.

The time-dependent coupled master equations, Eq. (5), are solved numerically by an implicit Euler method in discretizing the time derivative, followed by Newton's method to calculate the p_i's at the current time from those a time step earlier. The effect of the load resistance is taken into account in a similar way as in the 1D ME approach.

C. Three-dimensional Monte Carlo approach

It has recently been demonstrated that it is feasible to perform 3D MC simulations to study stationary charge transport in complete organic devices.[31,32] In these simulations it is possible to include Coulomb interactions explicitly. In the 3D ME approach this is not possible, because in that approach only average occupational probabilities are considered and thus only the effects of space charge can be accounted for. The 3D MC approach can therefore be applied as a check of the validity of the neglect of explicit Coulomb interactions in the 3D ME approach.

In the 3D MC approach the same cubic lattice of sites and the same hopping rate (Miller-Abrahams) is considered as in the 3D ME approach. However, now explicit hop events are chosen according to their rates and therefore the approach simulates what would actually happen in a real device. After every hop a charge moves and the 3D electric potential changes, requiring an update of all hopping rates. This makes the approach computationally expensive, although this can be mitigated by updating only hopping rates of charges in a sphere around the charge that hopped.[31] In our case a sphere radius of $8a$ turned out to be sufficient.

It is straightforward to extend the stationary 3D MC simulations of Ref. 31 to study transients. The now time-dependent current density is simply calculated by counting the net number of charges in the device that have hopped in the x direction in a certain time interval. This interval should be smaller than the time scale of the features appearing in the transients, but large enough to obtain sufficient statistics. The transients can be well captured by taking time intervals that grow exponentially with time. Taking into account the effect of the load resistance in the 3D MC simulations is cumbersome, so we refrained from doing that in the comparison with the 3D ME calculations.

IV. MODELING RESULTS AND COMPARISON WITH EXPERIMENT

Before the DI transients can be modeled, the modeling parameters should be determined. We did this by first performing stationary 1D ME calculations and fitting the results to the J-V characteristics of Fig. 4. The parameters with which the best fits were obtained for the three devices are given in Table I. The fit parameters are, next to N_t and σ, the mobility μ_0 at vanishing electric field and charge-carrier concentration, and the built-in voltage V_{bi} (the work function difference between the PEDOT:PSS and the Pd electrode). Excellent fits (blue dotted lines) to the experimental J-V curves are obtained with parameters that are compatible with the parameters determined in the earlier analysis of exactly the same devices in Refs. 11

TABLE I. Simulation parameters used in the 1D and 3D ME calculations, based on fits to the experimental J-V characteristics of Fig. 4. The results of earlier work (Refs. 11 and 29) are also given. The parameter values for ν_0 in the bottom part of the table apply to 3D ME calculations with a disorder strength σ that has been reduced to 0.08 eV. All other parameters of these calculations are the same as in the top part.

Parameter	This work	Earlier work[a]
N_t [10^{26} m^{-3}]	4.28	6 ± 1
σ [eV]	0.12	0.13 ± 0.01
$\nu_0^{67\,\mathrm{nm}}$ [10^{18} s]	4.7	
$\nu_0^{98\,\mathrm{nm}}$ [10^{18} s]	2.8	
$\nu_0^{122\,\mathrm{nm}}$ [10^{18} s]	2.8	
$\mu_0^{67\,\mathrm{nm}}$ [10^{-12} m^2/Vs]	6.3	5 ± 2
$\mu_0^{89\,\mathrm{nm}}$ [10^{-12} m^2/Vs]	4.2	5 ± 2
$\mu_0^{122\,\mathrm{nm}}$ [10^{-12} m^2/Vs]	4.3	5 ± 2
$V_{\mathrm{bi}}^{67\,\mathrm{nm}}$ [V]	1.57	1.66 ± 0.05
$V_{\mathrm{bi}}^{98\,\mathrm{nm}}$ [V]	1.54	1.63 ± 0.05
$V_{\mathrm{bi}}^{122\,\mathrm{nm}}$ [V]	1.80	1.87 ± 0.05
σ [eV]	0.08	
$\nu_0^{67\,\mathrm{nm}}$ [10^{16} s]	8.2	
$\nu_0^{98\,\mathrm{nm}}$ [10^{16} s]	4.9	
$\nu_0^{122\,\mathrm{nm}}$ [10^{16} s]	4.9	

[a]References 11 and 29.

and 29. Slightly different fabrication conditions between the three devices could have led to the slight differences in μ_0 and V_{bi}. With the parameters of Table I, also excellent fits to the experimental J-V curves can be obtained with stationary 3D ME simulations (green dashed lines), providing values for the intrinsic hopping rates ν_0 in Eq. (4). The value for the lattice constant a is obtained from N_t in this table as $a = 1/N_t^{1/3} = 1.33$ nm.

The predictions for the peak times from the Many-Rakavy theory, $t_{\mathrm{peak}} = 0.786L^2/\mu_0 V$,[22] obtained with the values for μ_0 in Table I, are plotted in Fig. 3 (gray lines). Clearly, the Many-Rakavy theory is unable to predict the correct peak times: they are more than an order of magnitude too large and their voltage dependence is too weak. This is not a surprise, because the Many-Rakavy theory does not take into account the mobility-enhancing effects of nonzero carrier densities and electric fields.

Including the time dependence, the DI transients can be obtained with the 1D ME approach, using the parameters in Table I, with, in particular, a disorder strength $\sigma = 0.12$ eV. The results are plotted in Figs. 1(c) and 2 (blue dotted lines), and the resulting peak times are plotted in Fig. 3 (blue squares). Three observations can be made: (1) the prediction of the peak times is considerably improved with respect to the Many-Rakavy theory, but they are still too large by about a factor of 3, and (2) the voltage dependence of the peak times is right; however, (3) the shape of the transients is not in agreement with experiment. In particular, the predicted structures (the depression before the peak and the peak itself) are too pronounced. The dependence of the mobility on carrier concentration and electric field in the 1D ME approach has led to an improvement as compared to the Many-Rakavy theory, but the agreement with experiment is still far from satisfactory. The still-too-large peak times should be attributed to the absence of carrier relaxation. At the start of the voltage pulse, carriers with high energy are injected into the device that initially have a larger mobility than when they have relaxed. This effect is not accounted for in the 1D ME approach.

With the 3D ME approach these carrier-relaxation effects are included. The green dashed lines in Figs. 1(c) and 2 show the transients obtained with the 3D ME approach, using the parameters in Table I. Instead of showing a maximum, the transients show a continuous decrease, with sometimes a shoulder present [indicated by the circle in Fig. 1(c), but not visible in all transients of Fig. 2] at a time that may be better in agreement with the experimental peak time than the peak time obtained with the 1D ME approach. Nevertheless, it is clear that with the value $\sigma = 0.12$ eV from Table I, the agreement with experiment is still not satisfactory.

To check a possible failing of the 3D ME approach due to its neglect of explicit Coulomb interactions, we made a comparison with 3D MC simulations. It turned out to be feasible to perform 3D MC simulations of the DI transients for the thinnest device with $L = 67$ nm at a relatively high pulse amplitude of 5 V. The comparison with the 3D ME transients is shown in Fig. 5. The agreement is very good, from which we can conclude that the 3D ME transients are reliable. For thicker devices and lower voltages the charge-carrier density will only be smaller, so that the effects of Coulomb interactions will be even smaller. We note that there is now no shoulder visible in the transients. The reason is the relatively large voltage over a thin device that we had to use in order to reach a sufficiently large signal-to-noise ratio in the MC simulations. This washes out structures in the transients.

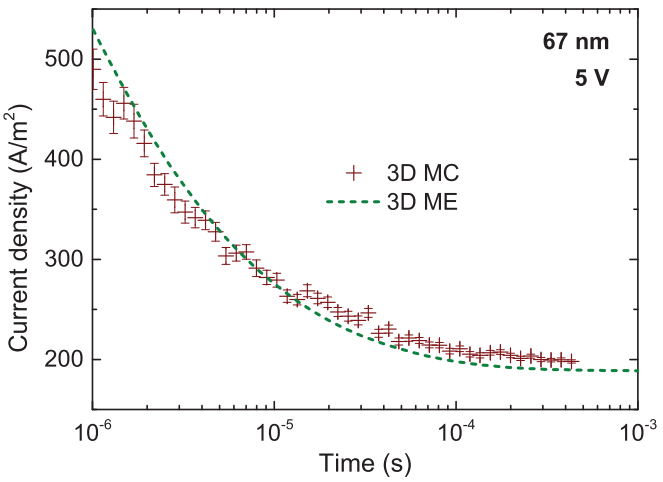

FIG. 5. (Color online) Comparison of the DI transient obtained with the 3D ME approach with that obtained with the 3D Monte Carlo (MC) approach, for the device with $L = 67$ nm, a pulse amplitude of 5 V, and $\sigma = 0.12$ eV. The load resistance is not included. The error bars in the 3D MC results are shown. In the 3D MC simulations explicit effects of Coulomb interactions between the charge carriers are included, but not in the 3D ME calculations. No shoulder is in this case visible in the transients.

We attribute the disappearance of the peak in the DI transients calculated with the 3D ME approach for $\sigma = 0.12$ eV to too-strong dispersive effects in the calculations. Dispersive transport leads to a spread in carrier transit times that will wash out features in the transients. To investigate this we decided to deviate from the value of σ found from the fitting of the 1D ME J-V curves and to explore lower values of σ that lead to less dispersion. We tried values of σ between 0.01 and 0.13 eV in steps of 0.01 eV and found that with $\sigma = 0.08$ eV the DI transients agree quite well with experiment [red dash-dotted lines in Figs. 1(c) and 2], with peak times (red triangles in Fig. 3) that accurately follow the experimental peak times. Since a smaller σ requires an adjustment of the intrinsic hopping rates ν_0 in Eq. (4) to arrive at the same mobility, we adjusted these rates to obtain a best fit of the 3D ME J-V curves (red dash-dotted lines in Fig. 4) to the measured curves. The new values found for ν_0 are given in the bottom part of Table I. We observe from Fig. 4 that the J-V curves obtained with $\sigma = 0.8$ eV still agree quite well with the experimental curves. Hence, a consistent picture seems to emerge from this analysis.

V. SUMMARY, DISCUSSION, AND CONCLUSION

We performed and analyzed room-temperature DI experiments on hole-only devices of a polyfluorene-based polymer with three different layer thicknesses. The current-density voltage (J-V) characteristics of these devices have been thoroughly investigated in terms of the EGDM. The DI transients show a peak that signals the arrival at the collecting contact of carriers injected by the injecting contact at the moment of the onset of a voltage pulse. A 1D ME approach that takes into account the dependence of the mobility on the carrier density and electric field provides an improvement of the prediction of the time at which the peak appears over the Many-Rakavy theory, which assumes a constant mobility. The used parameters are obtained from fits to the J-V characteristics. Because carrier-relaxation effects are not included in the 1D ME approach, the peak time is still significantly too large. With a 3D ME approach that does account for relaxation the peak changes into a shoulder that appears approximately at the experimental peak time. The disappearance of the peak is attributed to too-strong dispersive effects caused by the energetic disorder. With a somewhat reduced disorder strength σ, from 0.12 to 0.08 eV, the peak reappears and occurs at the correct time for the investigated devices and pulse amplitudes, while a satisfactory fit to the J-V characteristics is still possible.

It is clear from this work that the investigation of nonstationary charge transport in DI experiments provides an angle of view on charge transport in disordered organic semiconductors that is complementary to that provided by the investigation of stationary transport in J-V characteristics. From both angles of view, information about the disorder strength σ is obtained. An important question is now which of the two obtained values of σ is the appropriate one: the value of 0.12 eV obtained from the J-V characteristics or the value of 0.08 eV that appears to be compatible with the DI transients?

A possible answer to this question is that both values of σ are valid but apply to different parts of the DOS. It is possible that the assumption that the density of states can be described as a Gaussian with one standard deviation is too simple. In the stationary transport that determines the J-V characteristics, charge carriers have relaxed and probe the tail of the DOS, while during the relaxation in the nonstationary DI experiments charge carriers probe a much larger part of the DOS. This could lead to different apparent values of σ.

Another possible answer is that the value $\sigma = 0.08$ eV obtained from the DI experiments is the appropriate one. We have seen (Fig. 4) that also with this value a very satisfactory description of the J-V characteristics of the three devices can be obtained at room temperature. However, the larger value $\sigma = 0.12$ eV is compatible with the temperature dependence of the mobility,[12] which was modeled by a factor $\exp[-C(\sigma/k_{\mathrm{B}}T)^2]$, with a value $C = 0.39$ that falls in the range of $C = 0.38$–0.46, expected for disordered organic semiconductors.[33] In contrast, for $\sigma = 0.08$ eV the value needed for C ($\approx$0.9) would be considerably outside this range. A possible solution could be that the Miller-Abrahams hopping rate Eq. (4) is inappropriate. It was found that with Marcus hopping rates, which could be more appropriate in systems with considerable reorganization of the nuclear system upon charging or decharging, the temperature dependence can also be described by a factor $\exp[-C(\sigma/k_{\mathrm{B}}T)^2]$, but with a value of C that depends on the reorganization energy and can exceed the range mentioned above.[34]

The main conclusion of this work is that the consideration of relaxation effects in disordered organic semiconductors in dark-injection experiments provides an important additional tool to investigate charge transport in these semiconductors and has reopened the discussion about the appropriate model for charge transport.

ACKNOWLEDGMENTS

The authors thank Dr. R. J. de Vries, H. van Eersel, and A. Massé for important discussions. The research was supported by the Dutch nanotechnology program NanoNextNL (M.M.) and the Dutch Polymer Institute (DPI), Project No. 680 (J.C.).

[1] H. Bässler, Phys. Status Solidi B **175**, 15 (1993).
[2] Y. Roichman and N. Tessler, Synth. Met. **135**, 443 (2003).
[3] C. Tanase, E. J. Meijer, P. W. M. Blom, and D. M. de Leeuw, Phys. Rev. Lett. **91**, 216601 (2003).
[4] O. Rubel, S. D. Baranovskii, P. Thomas, and S. Yamasaki, Phys. Rev. B **69**, 014206 (2004).
[5] W. F. Pasveer, J. Cottaar, C. Tanase, R. Coehoorn, P. A. Bobbert, P. W. M. Blom, D. M. de Leeuw, and M. A. J. Michels, Phys. Rev. Lett. **94**, 206601 (2005).
[6] Y. Gartstein and E. Conwell, Chem. Phys. Lett. **245**, 351 (1995).
[7] S. V. Novikov, D. H. Dunlap, V. M. Kenkre, P. E. Parris, and A. V. Vannikov, Phys. Rev. Lett. **81**, 4472 (1998).

[8]M. Bouhassoune, S. van Mensfoort, P. Bobbert, and R. Coehoorn, Org. Electron. **10**, 437 (2009).
[9]S. L. M. van Mensfoort, V. Shabro, R. J. de Vries, R. A. J. Janssen, and R. Coehoorn, J. Appl. Phys. **107**, 113710 (2010).
[10]S. van Mensfoort, R. de Vries, V. Shabro, H. Loebl, R. Janssen, and R. Coehoorn, Org. Electron. **11**, 1408 (2010).
[11]S. L. M. van Mensfoort, S. I. E. Vulto, R. A. J. Janssen, and R. Coehoorn, Phys. Rev. B **78**, 085208 (2008).
[12]S. L. M. van Mensfoort, J. Billen, S. I. E. Vulto, R. A. J. Janssen, and R. Coehoorn, Phys. Rev. B **80**, 033202 (2009).
[13]H. Scher and E. W. Montroll, Phys. Rev. B **12**, 2455 (1975).
[14]G. Pfister, Phys. Rev. B **16**, 3676 (1977).
[15]T. Kreouzis, D. Poplavskyy, S. M. Tuladhar, M. Campoy-Quiles, J. Nelson, A. J. Campbell, and D. D. C. Bradley, Phys. Rev. B **73**, 235201 (2006).
[16]B. Movaghar, M. Grünewald, B. Ries, H. Bassler, and D. Würtz, Phys. Rev. B **33**, 5545 (1986).
[17]P. M. Borsenberger, L. T. Pautmeier, and H. Bässler, Phys. Rev. B **46**, 12145 (1992).
[18]W. C. Germs, J. J. M. van der Holst, S. L. M. van Mensfoort, P. A. Bobbert, and R. Coehoorn, Phys. Rev. B **84**, 165210 (2011).
[19]D. Poplavskyy and J. Nelson, J. Appl. Phys. **93**, 341 (2003).
[20]D. Poplavskyy, W. Su, and F. So, J. Appl. Phys. **98**, 014501 (2005).
[21]D. Poplavskyy and F. So, J. Appl. Phys. **99**, 033707 (2006).
[22]A. Many and G. Rakavy, Phys. Rev. **126**, 1980 (1962).
[23]E. Knapp and B. Ruhstaller, Opt. Quantum Electron. **42**, 667 (2011).
[24]Y. Roichman and N. Tessler, Appl. Phys. Lett. **80**, 1948 (2002).
[25]E. Knapp and B. Ruhstaller, J. Appl. Phys. **112**, 024519 (2012).
[26]R. Coehoorn and S. L. M. van Mensfoort, Phys. Rev. B **80**, 085302 (2009).
[27]M. Z. Szymanski, B. Luszczynska, and D. Djurado, IEEE J. Sel. Topics Quantum Electron. **19**, 7800107 (2013).
[28]J. J. M. van der Holst, M. A. Uijttewaal, B. Ramachandhran, R. Coehoorn, P. A. Bobbert, G. A. de Wijs, and R. A. de Groot, Phys. Rev. B **79**, 085203 (2009).
[29]R. J. de Vries, S. L. M. van Mensfoort, R. A. J. Janssen, and R. Coehoorn, Phys. Rev. B **81**, 125203 (2010).
[30]A. Miller and E. Abrahams, Phys. Rev. **120**, 745 (1960).
[31]J. J. M. van der Holst, F. W. A. van Oost, R. Coehoorn, and P. A. Bobbert, Phys. Rev. B **83**, 085206 (2011).
[32]M. Mesta, M. Carvelli, R. J. de Vries, H. van Eersel, J. J. M. van der Holst, M. Schober, M. Furno, B. Lüssem, K. Leo, P. Loebl, R. Coehoorn, and P. A. Bobbert, Nat. Mater. **12**, 652 (2013).
[33]R. Coehoorn, W. F. Pasveer, P. A. Bobbert, and M. A. J. Michels, Phys. Rev. B **72**, 155206 (2005).
[34]J. Cottaar, L. J. A. Koster, R. Coehoorn, and P. A. Bobbert, Phys. Rev. Lett. **107**, 136601 (2011).